

QCD-based charge symmetry breaking interaction and the Okamoto-Nolen-Schiffer anomaly

Hiroyuki Sagawa (佐川弘幸)^{1,2} Tomoya Naito (内藤智也)^{3,4} Xavier Roca-Maza^{5,6,7} and Tetsuo Hatsuda (初田哲男)³

¹RIKEN Nishina Center for Accelerator-based Science, Wako 351-0198, Japan

²Center for Mathematics and Physics, University of Aizu, Aizu-Wakamatsu, Fukushima 965-8560, Japan


³RIKEN Interdisciplinary Theoretical and Mathematical Sciences Program (iTHEMS), Wako 351-0198, Japan

⁴Department of Physics, Graduate School of Science, The University of Tokyo, Tokyo 113-0033, Japan

⁵Departament de Física Quàntica i Astrofísica and Institut de Ciències del Cosmos, Universitat de Barcelona, Martí i Franqués 1, 08028 Barcelona, Spain

⁶Dipartimento di Fisica, Università degli Studi di Milano, Via Celoria 16, 20133 Milano, Italy

⁷INFN, Sezione di Milano, Via Celoria 16, 20133 Milano, Italy

 (Received 30 May 2023; revised 16 October 2023; accepted 22 December 2023; published 25 January 2024)

An approach is proposed to link the charge symmetry breaking (CSB) nuclear interaction and the low-energy constants in quantum chromodynamics (QCD) by matching the CSB effect in nuclear matter. The resulting CSB interaction is applied to study the Okamoto-Nolen-Schiffer anomaly, still lacking a satisfactory microscopic understanding, on the energy differences of mirror nuclei by taking ^{17}F - ^{17}O , ^{15}O - ^{15}N , ^{41}Sc - ^{41}Ca , and ^{39}Ca - ^{39}K as typical examples. The magnitude and sign of the QCD-based CSB interactions are found to resolve the anomaly successfully within theoretical uncertainties.

DOI: [10.1103/PhysRevC.109.L011302](https://doi.org/10.1103/PhysRevC.109.L011302)

An anomaly in the energy differences of mirror nuclei and isobaric analog states, not yet well understood from a microscopic point of view, was found more than 50 years ago and is called the Okamoto-Nolen-Schiffer (ONS) anomaly [1,2]. It was first reported by Okamoto for the ^3He - ^3H system, and Nolen and Schiffer made a systematic study from light to heavy nuclei within the framework of the independent-particle model to find that the theoretical values of the energy difference underestimate the experimental values by 3–9%. Extra corrections such as the finite proton size, the center-of-mass effect, the Thomas-Ehrman effect, the isospin impurity, the electromagnetic spin-orbit interaction, the proton-neutron mass difference in the kinetic energy, the core polarization effect, and the vacuum polarization, altogether explain only about 1% of the discrepancy [3].

A possible remaining source to fill the gap is the charge symmetry breaking (CSB) nuclear interaction [1,4–7]. Recently, phenomenological CSB interactions (often taken to be a Skyrme-type contact interaction) have been introduced to systematically calculate the isospin symmetry breaking effect on top of the Coulomb interaction; they provide successful results for describing the isobaric analog states, the mass differences of isodoublet and isotriplet nuclei, and also the double- β decays [8–14]. However, both the magnitude and the sign of the parameters in phenomenological CSB interactions have not been well determined. Meanwhile, microscopic calculations of observables sensitive to isospin symmetry breaking terms in the nuclear Hamiltonian have also become available [15,16] although CSB effects have not been isolated in detail.

The aim of this Letter is to provide a quantum chromodynamics (QCD)-based understanding of CSB by making a quantitative link between the Skyrme-type CSB interactions [10] and the CSB effect due to the u - d quark mass

difference in QCD [17–19]. First, we perform a matching of the phenomenological and QCD-based calculations on the binding-energy difference between the neutron and the proton in an infinite nuclear matter to constrain the sign and magnitude of the phenomenological CSB interactions. Then, the results are utilized to study the mass difference of mirror nuclei ΔE of $(N \pm 1, Z)$ and $(N, Z \pm 1)$ with the closed-shell core ($A = N + Z = 16$ and 40) based on the Hartree-Fock (HF) wave functions, aiming to see whether the ONS anomaly can be resolved microscopically. These examples are chosen to suitably isolate CSB effects with respect to those originating from charge independence breaking (CIB) and, thus, robustly test our approach.

Let us start with the binding-energy difference between the neutron and the proton $\Delta_{np}(\rho)$ in infinite nuclear matter ($N = Z$) with the baryon density ρ , as defined by a difference of the momentum independent part of the Lorentz-scalar self-energies. In the leading order of the u - d quark mass difference and the quantum electrodynamics (QED) effect, an approximate formula has been obtained from the QCD sum rules (QSR) [18]:

$$\Delta_{np}(\rho) \simeq C_1 G(\rho) - C_2, \quad (1a)$$

$$G(\rho) = \left(\frac{\langle \bar{q}q \rangle}{\langle \bar{q}q \rangle_0} \right)^{1/3}. \quad (1b)$$

Here, $\langle \bar{q}q \rangle$ and $\langle \bar{q}q \rangle_0$ are, respectively, the isospin averaged in-medium and in-vacuum chiral condensate. The coefficient C_1 is proportional to the u - d quark mass difference δm ,¹ through

¹The renormalization group invariant mass difference reads $\delta m \equiv m_d - m_u \simeq 3.6 \text{ MeV}$ [20].

TABLE I. The parameters k_1 and k_2 in Eq. (2) corresponding to the adopted $\sigma_{\pi N}$ value with $m_\pi = 135$ MeV, $m_N = 938$ MeV, and $f_\pi = 92.4$ MeV.

$\sigma_{\pi N}$ (MeV)	k_1	k_2
45 ± 15	-0.38 ± 0.13	0.0093 ± 0.0031

the isospin-breaking constant $\gamma \equiv \langle \bar{d}d \rangle_0 / \langle \bar{u}u \rangle_0 - 1$ as $C_1 = -a\gamma$ with a positive numerical constant a determined by the Borel QSR method [18]. On the other hand, C_2 is a constant originating both from δm and the QED effect, and is written as $C_2 = C_1 - \Delta_{np}(0)$, where experimental neutron-proton mass difference in the vacuum is denoted by $\Delta_{np}(0) = m_n - m_p \simeq 1.29$ MeV. Equation (1) is valid at low density $\rho < \rho_0 = 0.17 \text{ fm}^{-3}$ where the dimension-3 chiral condensate gives a dominant contribution in the operator product expansion in QSR. In the following, we take $C_1 = 5.24_{-1.21}^{+2.48}$ MeV, where the central value is obtained from $\gamma = -7.8 \times 10^{-3}$ [18] and the uncertainty is estimated from $\gamma = -(6-11.5) \times 10^{-3}$ [21]. Since the C_2 term is density independent, it is canceled out in the following analysis.

Equation (1) implies that $\Delta_{np}(\rho)$ tends to decrease in the nuclear medium associated with the partial restoration of chiral symmetry $G(\rho) < 1$. The in-medium chiral condensate in the leading order with the Fermi-motion correction has a universal form [22,23]

$$\frac{\langle \bar{q}q \rangle}{\langle \bar{q}q \rangle_0} \simeq 1 + k_1 \frac{\rho}{\rho_0} + k_2 \left(\frac{\rho}{\rho_0} \right)^{5/3}, \quad (2a)$$

$$k_1 = -\frac{\sigma_{\pi N} \rho_0}{f_\pi^2 m_\pi^2} < 0, \quad k_2 = -k_1 \frac{3k_{F0}^2}{10m_N^2} > 0, \quad (2b)$$

where $\sigma_{\pi N}$ is the π - N sigma term, m_π (m_N) is the pion (nucleon) mass, and f_π is the pion decay constant. The Fermi momentum of the symmetric nuclear matter at saturation is denoted by $k_{F0} = (3\pi^2 \rho_0/2)^{1/3} = 268$ MeV. Systematic calculations using the in-medium chiral perturbation theory shows that the full chiral corrections up to next-to-next-to-leading order over Eq. (2) is numerically small for $\rho < \rho_0$ [24] (see Fig. S.1 in Supplemental Material [25]). Alternative evaluation of the higher-order chiral corrections with the Δ -excitation [26] does not change this conclusion (see Fig. S.2 in Supplemental Material [25]). We note however that the values of $\sigma_{\pi N}$ have large uncertainty: On the basis of the present values of $\sigma_{\pi N}$ from the scattering data and the lattice QCD data ($N_f = 2$ and $2 + 1$) summarized in Fig. 47 of the FLAG Review 2021 [20], we employ a conservative estimation, $\sigma_{\pi N} = 45 \pm 15$ MeV. This value and the error happen to be similar to the old estimation in Ref. [27]. Corresponding values of $k_{1,2}$ are summarized in Table I. We note that the recent data from the pionic atoms [28] indicate that $\langle \bar{q}q \rangle / \langle \bar{q}q \rangle_0 (\rho = 0.58 \rho_0) = 0.77 \pm 0.02$ which is consistent with the value obtained from Eqs. (2a) and (2b).

We decompose the mass difference between mirror nuclei $\Delta E = E(Z+1, N) - E(Z, N+1)$ into the Coulomb HF contribution ΔE_C and the ONS anomaly δ_{ONS} as

$$\Delta E = \Delta E_C + \delta_{\text{ONS}}. \quad (3)$$

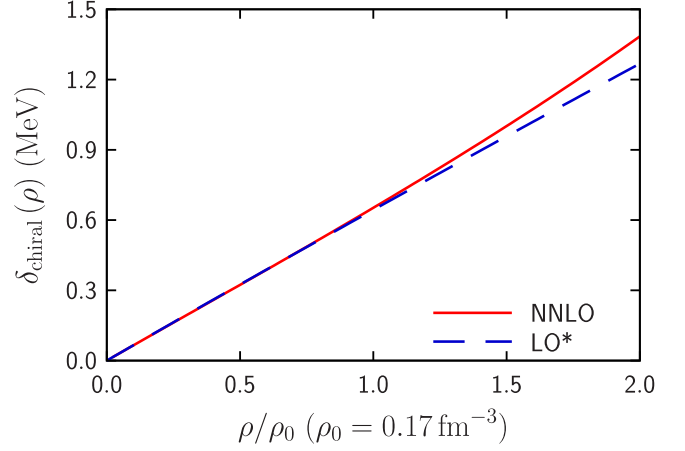


FIG. 1. The CSB effect from the partial restoration of chiral symmetry. Blue dashed curve (LO*): the leading-order formula with Fermi-motion correction [Eq. (2)]. Red curve: the NNLO result from in-medium chiral perturbation [24]. The central values of C_1 and $\sigma_{\pi N}$ are taken for these curves.

On the basis of Eq. (1), the CSB effect to δ_{ONS} from the partial restoration of chiral symmetry in the uniform and symmetric ($N = Z$) nuclear matter δ_{chiral} can be estimated as [18]

$$\delta_{\text{chiral}} \equiv \Delta_{np}(0) - \Delta_{np}(\rho) = C_1[1 - G(\rho)]. \quad (4)$$

Shown in Fig. 1 is δ_{chiral} as a function of the baryon density by taking the central values of C_1 and $\sigma_{\pi N}$ mentioned above. Two curves correspond to the LO result with the Fermi-motion correction (LO*) in Eq. (2) and the next-to-next-to-leading order (NNLO) result from the in-medium chiral perturbation [24]. The figure shows that Eq. (2) is quite accurate at least up to $\rho/\rho_0 \lesssim 1$. It should be noted here that δ_{chiral} is around a few hundreds keV for $\rho < \rho_0$, which is the right sign and magnitude to explain the ONS anomaly in finite nuclei.

Let us make an alternative evaluation of δ_{ONS} in Eq. (3) on the basis of the CSB interaction of an energy density functional (EDF). First of all, the general form of $E(Z, N)$ for uniform nuclear matter up to the second order of $\beta = (N - Z)/A$ reads [14]

$$\frac{E}{A} \simeq \varepsilon_0(\rho) + \varepsilon_1(\rho)\beta + \varepsilon_2(\rho)\beta^2. \quad (5)$$

In particular, for $N = Z$, we find the $\Delta E|_{N=Z} = -2\varepsilon_1(\rho)$ where the effect of ε_0 and ε_2 disappears. Note that ε_1 is a genuinely CSB-type term coming only from the CSB EDF. In this Letter, we take the Skyrme-type CSB interaction [10] to evaluate its contribution to $\varepsilon_1(\rho)$:

$$V_{\text{CSB}}(\mathbf{r}) = \left[s_0(1 + y_0 P_\sigma) \delta(\mathbf{r}) + \frac{s_1}{2}(1 + y_1 P_\sigma)(\mathbf{k}^{\dagger 2} \delta(\mathbf{r}) + \delta(\mathbf{r}) \mathbf{k}^2) + s_2(1 + y_2 P_\sigma) \mathbf{k}^\dagger \cdot \delta(\mathbf{r}) \mathbf{k} \right] \frac{\tau_{1z} + \tau_{2z}}{4}, \quad (6)$$

where $\tau_{iz} = +1$ (-1) for neutrons (protons) is the z direction of isospin operator of nucleon i , $\mathbf{k} = (\mathbf{V}_1 - \mathbf{V}_2)/2i$, $\mathbf{r} = \mathbf{r}_1 - \mathbf{r}_2$, and $P_\sigma = (1 + \boldsymbol{\sigma}_1 \cdot \boldsymbol{\sigma}_2)/2$ is the spin-exchange operator. In

TABLE II. Parameters of the Skyrme-type CSB interactions constrained from the low-energy constants in QCD. To evaluate the CSB effect in finite nuclei, where \tilde{s}_1 and \tilde{s}_2 contribute independently, two characteristic parameter sets (Cases I and II) are introduced.

	Case I	Case II
\tilde{s}_0 (MeV fm ³)	$-15.5^{+8.8}_{-12.5}$	$-15.5^{+8.8}_{-12.5}$
$\tilde{s}_1 + 3\tilde{s}_2$ (MeV fm ⁵)	$0.52^{+0.42}_{-0.29}$	0.00
\tilde{s}_1 (MeV fm ⁵)	$0.52^{+0.42}_{-0.29}$	0.00
\tilde{s}_2 (MeV fm ⁵)	0.00	$0.18^{+0.14}_{-0.10}$

Eq. (6), s_0 and y_0 are the strength parameters of the contact CSB and its spin exchange interactions, while s_1 (s_2) and y_1 (y_2) are the parameters of the momentum dependent s -wave (p -wave) CSB and its spin exchange interactions, respectively. Equation (6) gives contributions to $\varepsilon_1(\rho)$ and hence δ_{ONS} as [14]

$$\delta_{\text{Skyrme}} = -\frac{\tilde{s}_0}{4}\rho - \frac{1}{10}\left(\frac{3\pi^2}{2}\right)^{2/3}(\tilde{s}_1 + 3\tilde{s}_2)\rho^{5/3}, \quad (7)$$

where we have defined the effective coupling strengths,

$$\tilde{s}_0 \equiv s_0(1 - y_0), \quad \tilde{s}_1 \equiv s_1(1 - y_1), \quad \tilde{s}_2 \equiv s_2(1 + y_2). \quad (8)$$

Note that the Thomas-Fermi approximation is adopted to evaluate the kinetic energy terms in Eq. (5).

There have been attempts to extract $\tilde{s}_{0,1,2}$ by using various experimental data such as the energy of isobaric analog states (IAS) [8] and the mass differences of mirror and isotriplet nuclei [11]. The value of \tilde{s}_0 estimated from IAS in ²⁰⁸Pb is $\tilde{s}_0 = -52.6 \pm 1.4$ MeV fm³, while the mass differences of mirror nuclei lead to two estimates: $(\tilde{s}_0, \tilde{s}_{1,2}) = (-29.2 \pm 1.2$ MeV fm³, 0) and $(\tilde{s}_0, \tilde{s}_1, \tilde{s}_2) = (44 \pm 8$ MeV fm³, -56 ± 16 MeV fm⁵, -31.2 ± 3.2 MeV fm⁵).

The parameters in Ref. [11] are related to ours as $\tilde{s}_{0,1,2}^{\text{III}} = \tilde{s}_{0,1,2}/4$. Since the contributions of \tilde{s}_0 and $\tilde{s}_{1,2}$ tend to cancel each other in physical observables, it is rather difficult to determine the magnitude and the sign of each term only from the present experimental data.

On the other hand, our approach is to constrain $\tilde{s}_{0,1,2}$ from the low-energy constants in QCD, γ and $\sigma_{\pi N}$, by matching $\delta_{\text{Skyrme}}(\rho)$ in Eq. (7) and $\delta_{\text{chiral}}(\rho)$ expanded up to $\mathcal{O}(\rho^{5/3})$ at low densities. Then, we obtain

$$\tilde{s}_0 = -\frac{4 C_1 \sigma_{\pi N}}{3 f_{\pi}^2 m_{\pi}^2}, \quad \tilde{s}_1 + 3\tilde{s}_2 = \frac{1}{m_N^2} \frac{C_1 \sigma_{\pi N}}{f_{\pi}^2 m_{\pi}^2}. \quad (9)$$

The magnitudes and signs of \tilde{s}_0 and $\tilde{s}_1 + 3\tilde{s}_2$ are summarized in Table II, where the linear uncertainty estimation is used. To evaluate the CSB effect in finite nuclei, where \tilde{s}_1 and \tilde{s}_2 contribute independently, two characteristic parameter sets (Cases I and II) are introduced.

To carry out precise calculation of the mass differences of mirror nuclei, we consider two types of the Skyrme EDFs for the isospin symmetric part, SGII [32] and SAMi [33]; they reproduce well, within 0.3%, the experimental radii of the $N = Z$ closed shell nuclei, ¹⁶O and ⁴⁰Ca, as shown in Table III. It is important for any adopted EDF to reproduce the

TABLE III. The neutron radii, the proton ones, and the charge ones of ¹⁶O and ⁴⁰Ca. Two types of Skyrme EDFs, SGII, and SAMi, are adopted for the HF calculation. Experimental data are taken from Refs. [29–31].

¹⁶ O	r_n	r_p	r_c
SGII	2.601	2.626	2.744
SAMi	2.625	2.648	2.765
Expt. [29]	—	—	2.737
⁴⁰ Ca	r_n	r_p	r_c
SGII	3.325	3.374	3.467
SAMi	3.342	3.390	3.482
Expt. [30]	3.375	3.385	3.480
Expt. [31]	—	—	3.478

charge radii since the Coulomb energy part ΔE_C is essentially determined by the charge distribution: The change of 1% in the charge radius of ⁴⁰Ca gives rise to 20–30 keV difference in ΔE_C of mirror nuclei.

The contributions of the CSB interactions to the mass difference between mirror nuclei of $(N \pm 1, Z)$ and $(N, Z \pm 1)$ with the closed-shell core $A = N + Z = 16$ and 40 are calculated by using HF wave functions for SGII and SAMi. As we can see from the Table IV, \tilde{s}_0 provides a dominant contribution (210–320 keV), more than one order of magnitude larger than the $\tilde{s}_{1(2)}$ contributions. The net results are slightly different from the sum of \tilde{s}_0 and $\tilde{s}_{1(2)}$ contributions due to the nonlinear effect in the calculation using EDFs. The final results of Case I and those of Case II are essentially identical due to the \tilde{s}_0 dominance, so that we focus on Case I below.

Let us now turn to the comparison of the theoretical values with our CSB interaction with the experimental mass difference of the mirror nuclei by including ΔE_C and other extra

TABLE IV. Contributions from the Skyrme CSB interactions to δ_{ONS} in Cases I and II with theoretical uncertainties. The values are given in unit of keV. The core density and the wave function of valence orbit are calculated by HF model with Skyrme EDFs, SGII, and SAMi. All the values are obtained self-consistently.

Nuclei	¹⁷ F - ¹⁷ O	¹⁵ O - ¹⁵ N	⁴¹ Sc - ⁴¹ Ca	³⁹ Ca - ³⁹ K	
Orbital	$1d_{5/2}$	$(1p_{1/2})^{-1}$	$1f_{7/2}$	$(1d_{3/2})^{-1}$	
SGII	\tilde{s}_0	229^{+192}_{-125}	269^{+221}_{-148}	292^{+245}_{-160}	322^{+264}_{-176}
	\tilde{s}_1 ($\tilde{s}_2 = 0$)	$-5.0^{+2.8}_{-4.0}$	$-5.6^{+3.1}_{-4.5}$	$-6.6^{+3.7}_{-5.3}$	$-6.0^{+3.4}_{-4.9}$
	\tilde{s}_2 ($\tilde{s}_1 = 0$)	$-6.4^{+3.5}_{-5.2}$	$-3.3^{+1.8}_{-2.7}$	$-5.3^{+2.9}_{-4.3}$	$-5.0^{+2.8}_{-4.1}$
	Case I	224^{+192}_{-125}	264^{+221}_{-148}	287^{+245}_{-160}	315^{+264}_{-176}
	Case II	225^{+192}_{-125}	266^{+221}_{-148}	289^{+245}_{-160}	316^{+264}_{-176}
SAMi	\tilde{s}_0	211^{+174}_{-115}	274^{+225}_{-152}	278^{+230}_{-151}	324^{+269}_{-180}
	\tilde{s}_1 ($\tilde{s}_2 = 0$)	$-5.2^{+2.9}_{-4.2}$	$-5.4^{+3.0}_{-4.4}$	$-7.3^{+4.0}_{-5.9}$	$-8.4^{+4.6}_{-6.6}$
	\tilde{s}_2 ($\tilde{s}_1 = 0$)	$-4.1^{+2.3}_{-3.3}$	$-3.2^{+1.8}_{-2.6}$	$-5.7^{+3.1}_{-4.6}$	$-5.2^{+2.9}_{-4.2}$
	Case I	206^{+174}_{-115}	269^{+225}_{-152}	271^{+230}_{-151}	321^{+269}_{-180}
	Case II	207^{+174}_{-115}	271^{+225}_{-152}	272^{+230}_{-151}	322^{+269}_{-180}

TABLE V. The breakdown of the mass differences of mirror nuclei ΔE into each contribution Coulomb, Extra, and CSB interaction (CSBI) for Case I with the Skyrme EDF, SGII. Numbers are given in units of MeV.

Nuclei	$^{17}\text{F} - ^{17}\text{O}$	$^{15}\text{O} - ^{15}\text{N}$	$^{41}\text{Sc} - ^{41}\text{Ca}$	$^{39}\text{Ca} - ^{39}\text{K}$
Orbital	$1d_{5/2}$	$(1p_{1/2})^{-1}$	$1f_{7/2}$	$(1d_{3/2})^{-1}$
ΔE_D (Coulomb)	3.596	3.272	7.133	6.717
ΔE_E (Coulomb)	-0.203	0.026	-0.267	0.260
Extra	0.040	0.028	0.102	0.011
CSBI (Case I)	0.224	0.264	0.287	0.315
Sum (without CSBI)	3.432	3.326	6.965	6.985
Sum (with CSBI)	3.656	3.590	7.252	7.300
Expt. [36]	3.543	3.537	7.278	7.307

contributions [6,8,34,35] (see Supplemental Material [25]). The results are summarized in Table V for SGII and Table VI for SAMi assuming Case I. First, we note that the core density and the wave function of valence orbital are calculated with the closed shell core configuration without the core polarization effect of the valence nucleon. The direct and exchange contributions of the Coulomb interaction (ΔE_D and ΔE_E with $\Delta E_C = \Delta E_D + \Delta E_E$) are obtained with the exact treatment of the exchange term. The sum of extra contributions including the finite-size effect of nucleon, the center-of-mass effect on nuclear density, the Thomas-Ehrman effect δ_{NN}^1 , the isospin impurity δ_{NN}^2 , the electromagnetic spin-orbit interaction, the core polarization effect of the last nucleon, the proton and neutron mass difference in the kinetic energy, and the vacuum polarization, are listed as ‘‘Extra’’ in the Tables V and VI: Each contribution varies from -150 keV to 150 keV, while the net result is at most 100 keV due to a strong cancellation. See Supplemental Material [25] for the details.

The sum of ΔE_D , ΔE_E , and Extra denoted by ‘‘Sum (without CSBI)’’ in the tables is systematically smaller than the experimental value by 3–6%. Our CSBI contributions constrained by the low-energy constants in QCD fill the gap as it can be seen by comparing the sum neglecting CSBI effects, the sum containing CSBI effects ‘‘Sum (with CSBI)’’ and the experimental (‘‘Expt.’’) rows in Tables V and VI. Shown in Fig. 2 is $\delta_{\text{ONS}} = \Delta E - \Delta E_C$, where it is evident the agreement between experiment and the present theoretical estimates. The

TABLE VI. The same as Table V, but with the Skyrme EDF, SAMi.

Nuclei	$^{17}\text{F} - ^{17}\text{O}$	$^{15}\text{O} - ^{15}\text{N}$	$^{41}\text{Sc} - ^{41}\text{Ca}$	$^{39}\text{Ca} - ^{39}\text{K}$
Orbital	$1d_{5/2}$	$(1p_{1/2})^{-1}$	$1f_{7/2}$	$(1d_{3/2})^{-1}$
ΔE_D (Coulomb)	3.506	3.242	7.025	6.697
ΔE_E (Coulomb)	-0.193	0.022	-0.259	0.281
Extra	0.043	0.075	0.104	0.092
CSBI (Case I)	0.206	0.269	0.271	0.321
Sum (without CSBI)	3.356	3.339	6.870	7.070
Sum (with CSBI)	3.562	3.608	7.141	7.391
Expt. [36]	3.543	3.537	7.278	7.307

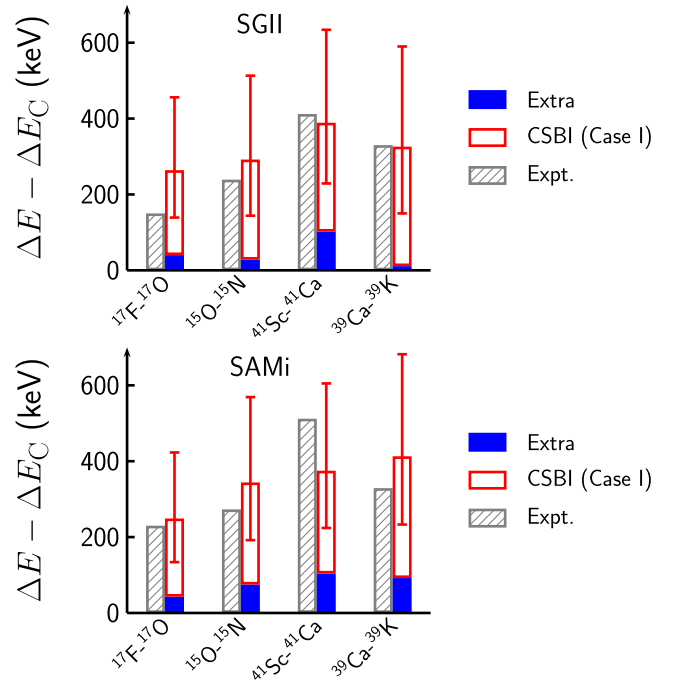


FIG. 2. Comparisons of the experimental ONS anomaly $\Delta E_{\text{Expt.}} - \Delta E_C$ (grey hatched bars) and the corresponding theoretical estimates in two EDFs (SGII and SAMi). The contribution from the QCD-based CSB interaction (CSBI) in Case I and the extra contributions are indicated by the red bars with error bars and the blue bars, respectively.

theoretical error bars given in Table IV are shown in the figure, while the experimental error bars are around only 5 keV and would not be visible in the scale of the figure.

Finally, as mentioned, there has been a recent effort in quantifying the effects of CSB in some selected nuclear observables [8,9,11,15,37]. However, depending on the theoretical method employed, the estimated central values of the leading order term CSB parameter (\tilde{s}_0) can differ by one order of magnitude among the different approaches and could even be of different sign (cf. Ref. [38] and Supplemental Material [25]).

In summary, we evaluated the EDF parameters of Skyrme-type CSB interactions, not only the contact term (\tilde{s}_0) but also the momentum-dependent terms ($\tilde{s}_{1,2}$), by utilizing the low-energy constants in QCD and the density dependence of chiral condensation of $\bar{q}q$ pair in the nuclear medium for the first time. The resulting QCD-based CSB interaction is applied to resolve the ONS anomaly: The numerical results for the mirror nuclei ($A = 16 \pm 1$ and $A = 40 \pm 1$ with the isosymmetric core $N = Z = A/2$) with two Skyrme EDFs (SGII and SAMi) show good agreement with experimental data both in sign and magnitude within the theoretical error bars. Major theoretical uncertainty of the final results originates from the values of γ and $\sigma_{\pi N}$: Increasing the accuracy of these constants from the experimental data or from the lattice QCD simulations will be instrumental.

The QCD-based CSB interaction discussed in this Letter would have strong impact on isospin symmetry breaking phenomena such as IAS, the superallowed β decay in the context

of Cabibbo-Kobayashi-Maskawa unitary matrix, and the mass predictions of mirror and isotriplet nuclei near the proton drip line. We plan to make systematic studies of these quantities.

The authors thank Gianluca Colò and Toshio Suzuki for fruitful discussions. H.S. acknowledges the Grant-in-Aid for Scientific Research (C) under Grant No. 19K03858. T.N. acknowledges the RIKEN Special Postdoctoral Researcher

Program, the JSPS Grant-in-Aid for Research Activity Start-up under Grant No. 22K20372, the JSPS Grant-in-Aid for Transformative Research Areas (A) under Grant No. 23H04526, the JSPS Grant-in-Aid for Scientific Research (B) under Grant No. 23H01845, and the JSPS Grant-in-Aid for Scientific Research (C) under Grant No. 23K03426. T.H. was partially supported by JSPS Grant-in-Aid No. 18H05236.

-
- [1] K. Okamoto, Coulomb energy of ${}^3\text{He}$ and possible charge asymmetry of nuclear forces, *Phys. Lett.* **11**, 150 (1964).
- [2] J. A. Nolen, Jr. and J. P. Schiffer, Coulomb energies, *Annu. Rev. Nucl. Sci.* **19**, 471 (1969).
- [3] S. Shlomo, Nuclear Coulomb energies, *Rep. Prog. Phys.* **41**, 957 (1978).
- [4] J. W. Negele, The ${}^{41}\text{Sc}$ - ${}^{41}\text{Ca}$ Coulomb energy difference, *Nucl. Phys. A* **165**, 305 (1971).
- [5] P. G. Blunden and M. J. Iqbal, Relativistic Hartree-Fock calculations for finite nuclei, *Phys. Lett. B* **196**, 295 (1987).
- [6] T. Suzuki, H. Sagawa, and A. Arima, Effects of valence nucleon orbits and charge symmetry breaking interaction on the Nolen-Schiffer anomaly of mirror nuclei, *Nucl. Phys. A* **536**, 141 (1992).
- [7] G. A. Miller, B. M. K. Nefkens, and I. Slaus, Charge symmetry, quarks and mesons, *Phys. Rep.* **194**, 1 (1990).
- [8] X. Roca-Maza, G. Colò, and H. Sagawa, Nuclear symmetry energy and the breaking of the isospin symmetry: How do they reconcile with each other?, *Phys. Rev. Lett.* **120**, 202501 (2018).
- [9] P. Bączyk, J. Dobaczewski, M. Konieczka, W. Satuła, T. Nakatsukasa, and K. Sato, Isospin-symmetry breaking in masses of $N \simeq Z$ nuclei, *Phys. Lett. B* **778**, 178 (2018).
- [10] H. Sagawa, G. Colò, X. Roca-Maza, and Y. Niu, Collective excitations involving spin and isospin degrees of freedom, *Eur. Phys. J. A* **55**, 227 (2019).
- [11] P. Bączyk, W. Satuła, J. Dobaczewski, and M. Konieczka, Isobaric multiplet mass equation within nuclear density functional theory, *J. Phys. G* **46**, 03LT01 (2019).
- [12] T. Naito, G. Colò, H. Liang, X. Roca-Maza, and H. Sagawa, Toward *ab initio* charge symmetry breaking in nuclear energy density functionals, *Phys. Rev. C* **105**, L021304 (2022).
- [13] T. Naito, X. Roca-Maza, G. Colò, H. Liang, and H. Sagawa, Isospin symmetry breaking in the charge radius difference of mirror nuclei, *Phys. Rev. C* **106**, L061306 (2022).
- [14] T. Naito, G. Colò, H. Liang, X. Roca-Maza, and H. Sagawa, Effects of Coulomb and isospin symmetry breaking interactions on neutron-skin thickness, *Phys. Rev. C* **107**, 064302 (2023).
- [15] S. J. Novario, D. Lonardonì, S. Gandolfi, and G. Hagen, Trends of neutron skins and radii of mirror nuclei from first principles, *Phys. Rev. Lett.* **130**, 032501 (2023).
- [16] R. B. Wiringa (private communication).
- [17] E. M. Henley and G. Krein, Nambu–Jona-Lasinio model and charge independence, *Phys. Rev. Lett.* **62**, 2586 (1989).
- [18] T. Hatsuda, H. Høgaasen, and M. Prakash, QCD sum rules in medium and the Okamoto-Nolen-Schiffer anomaly, *Phys. Rev. Lett.* **66**, 2851 (1991).
- [19] K. Saito and A. W. Thomas, The Nolen-Schiffer anomaly and isospin symmetry breaking in nuclear matter, *Phys. Lett. B* **335**, 17 (1994).
- [20] Y. Aoki *et al.* [Flavour Lattice Averaging Group (FLAG)], FLAG review 2021, *Eur. Phys. J. C* **82**, 869 (2022).
- [21] S. Narison, *QCD as a Theory of Hadrons*, Cambridge Monographs on Particle Physics, Nuclear Physics and Cosmology (Cambridge University Press, Cambridge, 2004).
- [22] R. S. Hayano and T. Hatsuda, Hadron properties in the nuclear medium, *Rev. Mod. Phys.* **82**, 2949 (2010).
- [23] P. Gubler and D. Satow, Recent progress in QCD condensate evaluations and sum rules, *Prog. Part. Nucl. Phys.* **106**, 1 (2019).
- [24] S. Goda and D. Jido, Chiral condensate at finite density using the chiral Ward identity, *Phys. Rev. C* **88**, 065204 (2013).
- [25] See Supplemental Material at <http://link.aps.org/supplemental/10.1103/PhysRevC.109.L011302> for the fitting procedure of the chiral-condensate as well as the numerical details of various contributions to the mass differences of mirror nuclei in the Hartree-Fock calculation [6,35].
- [26] N. Kaiser, P. de Homont, and W. Weise, In-medium chiral condensate beyond linear density approximation, *Phys. Rev. C* **77**, 025204 (2008).
- [27] J. Gasser, H. Leutwyler, and M. E. Sainio, Sigma term update, *Phys. Lett. B* **253**, 252 (1991).
- [28] T. Nishi, K. Itahashi, D. Ahn, G. P. A. Berg, M. Dozono, D. Etoh, H. Fujioka, N. Fukuda, N. Fukunishi, H. Geissel, E. Haettner, T. Hashimoto, R. S. Hayano, S. Hirenzaki, H. Horii, N. Ikeno, N. Inabe, M. Iwasaki, D. Kameda, K. Kisamori *et al.* (piAF Collaboration), Chiral symmetry restoration at high matter density observed in pionic atoms, *Nat. Phys.* **19**, 788 (2023).
- [29] H. De Vries, C. W. De Jager, and C. De Vries, Nuclear charge-density-distribution parameters from elastic electron scattering, *At. Data Nucl. Data Tables* **36**, 495 (1987).
- [30] J. Zenihiro *et al.*, Direct determination of the neutron skin thicknesses in ${}^{40,48}\text{Ca}$ from proton elastic scattering at $E_p = 295$ MeV, [arXiv:1810.11796](https://arxiv.org/abs/1810.11796) [nucl-ex] (2018).
- [31] G. Fricke and K. Heilig, *Nuclear Charge Radii 20-Ca Calcium: Datasheet from Landolt-Börnstein - Group I Elementary Particles, Nuclei and Atoms*, Vol. 20: “Nuclear Charge Radii” in SpringerMaterials (Springer-Verlag, Berlin/Heidelberg, 2004).
- [32] N. Van Giai and H. Sagawa, Spin-isospin and pairing properties of modified Skyrme interactions, *Phys. Lett. B* **106**, 379 (1981).
- [33] X. Roca-Maza, G. Colò, and H. Sagawa, New Skyrme interaction with improved spin-isospin properties, *Phys. Rev. C* **86**, 031306(R) (2012).

- [34] E. A. Uehling, Polarization Effects in the positron theory, *Phys. Rev.* **48**, 55 (1935).
- [35] N. Van Giai, D. Vautherin, M. Veneroni, and D. M. Brink, Coulomb energy differences in mirror nuclei in the Hartree-Fock approximation, *Phys. Lett. B* **35**, 135 (1971).
- [36] W. J. Huang, M. Wang, F. G. Kondev, G. Audi, and S. Naimi, The AME 2020 atomic mass evaluation (I). Evaluation of input data, and adjustment procedures, *Chin. Phys. C* **45**, 030002 (2021).
- [37] H. Sagawa, S. Yoshida, T. Naito, T. Uesaka, J. Zenihiro, J. Tanaka, and T. Suzuki, Isovector density and isospin impurity in ^{40}Ca , *Phys. Lett. B* **829**, 137072 (2022).
- [38] T. Naito, G. Colò, T. Hatsuda, H. Liang, X. Roca-Maza, and H. Sagawa, Possible inconsistency between phenomenological and theoretical determinations of charge symmetry breaking in nuclear energy density functionals, [arXiv:2309.17060](https://arxiv.org/abs/2309.17060) [nucl-th] (2023).